UV-written Integrated Optical 1xN Splitters

UV-written Integrated Optical 1×N Splitters

Massimo Olivero*, Mikael Svalgaard

COM, Technical University of Denmark, 2800 Lyngby, Denmark,
Phone: (+45) 4525 5748, Fax: (+45) 4593 6581,
svlgrd@com.dtu.dk

**Presently at PhotonLab, Politecnico di Torino, 10129 Torino, Italy,*
Phone: (+39) 011 2276301, Fax:(+39) 011 2276309,
massimo.olivero@polito.it

Abstract: The first demonstration of UV-written, silica-on-silicon integrated optical 1×N power splitters with up to 32 outputs ports is presented. The fabricated components exhibit 450 nm bandwidth, low excess loss and good channel uniformity.

OCIS codes: (250.5300) Photonic integrated circuits, (230.1360) Beam splitters, (130.3120) Integrated optics devices, (060.2340) Fiber optics components, (160.5320) Photorefractive materials, (230.7390) Waveguides, planar, (260.7190) Ultraviolet, (350.4600) Optical engineering.

References and Links

1. M. Svalgaard, C. V. Poulsen, A. Bjarklev, O. Poulsen, " UV-writing of buried single-mode channel waveguides in Ge-doped silica films,", Electron. Lett. **30**, 1401–1402 (1994).
2. M. Svalgaard, K. Færch, L. U. Andersen, "Variable Optical Attenuator Fabricated by Direct UV Writing," J. Lightwave Technol. **21–9**, 2097-2103 (2003).
3. C. Peucheret, Y. Geng, M. Svalgaard, B. Zsigri, H. R. Sørensen, N. Chi, H.-J. Deyerl, M. Kristensen, P. Jeppesen, "Direct UV written Michelson Interferometer for RZ Signal Generation Using Phase-to-Intensity Modulation Conversion," IEEE Photonics Technol. Lett. **17**, 1674-1676 (2005).
4. M. Olivero, M. Svalgaard, "Direct UV-written broadband directional planar waveguide couplers," Opt. Express **13**, 8390-8399 (2005).
5. Standards ITU-G 983.5 and ITU-G 983.6, 2002. Available: http://www.itu.int/rec/recommendation.asp?type=products&lang=e&parent=T-REC-G
6. G.D. Maxwell, B.J. Ainslie, "Demonstration of a directly written directional coupler using UV induced photosensitivity in a planar silica waveguide," Electron. Lett. **31**, 1694-1695 (1995).
7. D. Zauner, K. Kulstad, J. Rathje, M. Svalgaard, "Directly UV written silica–on–silicon planar waveguides with low insertion loss," Electron. Lett. **34**, 1582-1584 (1998).
8. P.J. Lemaire, R. M. Atkins, V. Mizrahi, W.A. Reed, "High pressure H2 loading as a technique for achieving ultrahigh UV photosensitivity and thermal sensitivity in GeO2 doped optical fibres," Electron. Lett. **29**, 1191-1193 (1993).
9. M. Svalgaard, "Effect of D_2 outdiffusion on direct UV writing of waveguides," Electron. Lett. **35**, 1840-1841 (1999).
10. Renishaw plc., New Mills, Wotton-under-Edge, Gloucestershire, GL12 8JR, United Kingdom, tutorial: http://www.renishaw.com/UserFiles/acrobat/UKEnglish/GEN-NEW-0117.pdf.
11. M. Svalgaard, A. Harpøth, M. Andersen, "The role of local heating in the formation process of UV written optical waveguides," Opt. Express **13**, 7823-7831 (2005).
12. R.A. Betts, F. Lui, T.W. Whitbread, "Non destructive two-dimensional refractive index profiling of integrated optical waveguides by an interferometric method," Appl. Opt. **30**, 4384-4389 (1991).
13. T. Erdogan, V. Mizrahi, P. J. Lemarie, D. Monroe, "Decay of ultra–violet–light induced Bragg gratings," J. Appl. Phys. **76**, 73-80 (1994).
14. M. Svalgaard, "Direct writing of planar waveguide power splitters and directional couplers using a focused ultraviolet laser beam," Electron. Lett. **33**, 1694-1695 (1997).
15. R. Syms, J. Cozens, "The slab waveguide-tapers," in *Optical Guided Waves and Devices*, (McGraw-Hill International Ltd., 1992), pp. 19-22.
16. K. Færch, M. Svalgaard, "Symmetrical waveguide device fabricated by direct UV writing," IEEE Photonics Technol. Lett. **14**, 173-175 (2002).

#9482 - $15.00 USD Received 15 November 2005; revised 19 December 2005; accepted 19 December 2005

17. M Olivero, M. Svalgaard, "UV written 1×8 optical splitters," in *Proceedings of OSA Topical Meeting on Bragg Gratings, Poling and Photosensitivity*, B.J. Eggleton, ed., (Technical Digest Series, Optical Society of America, Washington, D.C., 2005), 37-38.

1. Introduction

The need for compact and high-performance integrated waveguide components for optical telecommunication is steadily increasing. Standard waveguide fabrication techniques using photolithography and etching are capable of yielding high quality components, but the investments required to set up and operate the production facilities are quite large. An interesting alternative for low-cost production is the direct UV writing technique [1], where waveguides are fabricated by scanning a photosensitive glass sample under a focused ultraviolet (UV) beam. This process avoids the use of costly photolithographic and etching based fabrication steps and does not require a cleanroom. We have previously shown that direct UV writing can be a stable platform for production of high performance components such as variable optical attenuators [2], return-to-zero signal generators [3] and broadband directional couplers [4].

Low cost 1×N power splitters are considered to be enabling components for widespread deployment of Fiber-To-The-Home (FTTH) networks [5]. Such components often have a complicated circuit layout, with numerous branching points, and this places stringent requirements on the accuracy and reproducibility of a UV writing setup if good performance is to be achieved. In this paper we report the fabrication of 1×N splitters with N=4,8,16,32 output channels by means of UV writing. The circuit layout has been optimized for compactness, low loss and broadband operation. The performance in terms of size, loss and uniformity are close to or within current commercial specifications in the 1300–1750 nm wavelength range. To our best knowledge, the 1×N optical splitters reported here represent the largest and most advanced circuit layouts yet realized with the UV writing technique.

2. Experimental procedure

This study was conducted using three layer (buffer/core/cladding) silica-on-silicon samples with a photosensitive core layer. The buffer layer consists of thermal oxide while the core/cladding structure is deposited by plasma enhanced chemical vapor deposition. The thickness of the buffer/core/cladding layer is 16/5.4/12 μm. The core contains germanium and boron in a relative concentration so that the refractive index is matched (within $\pm 5\times10^{-4}$) to that of the surrounding layers [6]. Index matching the core layer enables the UV-written waveguides to exhibit a circular-mode profile and low coupling loss to standard telecom fiber [7]. Prior to UV exposure, the sample is loaded with molecular deuterium at a pressure of 500 bar until saturation to increase the photosensitivity [8].

The UV writing setup, similar to that used in previous work [4], is depicted in Fig.1. The beam of a frequency doubled Ar^+ laser producing 257 nm radiation is directed to a spatial filter / beam expander section and focused by a microscope objective on the sample with a $1/e^2$ spotsize of 3.1 μm and a Rayleigh range of 55 μm. A computer controlled shutter positioned in the beam path blocks the beam as required by the scanning process. During UV writing the sample is housed in a vacuum chamber where it is thermo-electrically cooled to −30 °C in order to reduce the deuterium outdiffusion rate [9]. Cooling of the sample increases the available UV writing time from ~15 min. at room temperature to more than 20 hours. Waveguides are written according to the desired layout by translating the sample chamber using computer controlled, high-precision x-y translation stages. The position of the sample chamber is monitored with 10 nm precision at a rate of 25 Hz using two double-step laser interferometers [10]. Interferometric position monitoring ensures a very high degree of scanning precision which is essential for the fabrication of extended components that require

#9482 - $15.00 USD Received 15 November 2005; revised 19 December 2005; accepted 19 December 2005

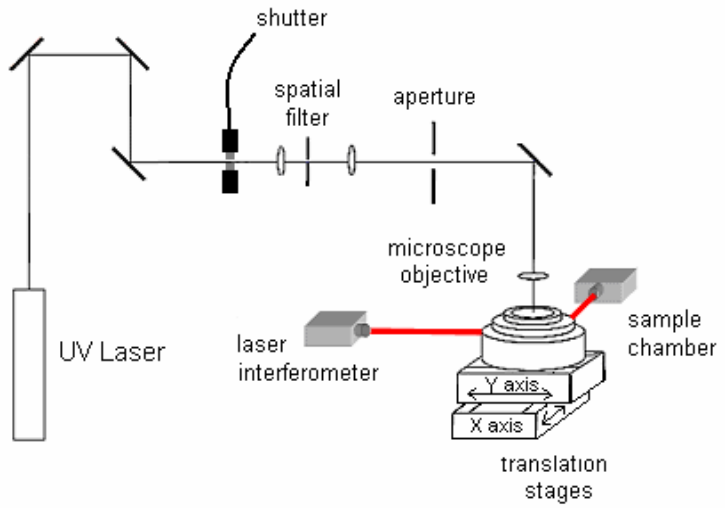

Fig.1. Schematic drawing of the setup used for direct UV writing

many concatenated scans, such as 1×N splitters. The UV power incident on the sample is set to 45 mW and a scan velocity of 280 μm/s is chosen for standard waveguide sections. This yields a stable index change process without discontinuities [11] and a waveguide width of 6.0 μm, as measured with differential interference contrast microscopy.

After UV writing the sample is annealed at 80 °C for 12 hours to outdiffuse residual deuterium without thermally inducing reactions with the glass matrix. After this annealing the peak index step is 0.014±0.0005, as measured by detecting interference fringes from the waveguide and its surrounding area upon illumination with semi−coherent light [12]. Single mode operation in both the 1.3 μm and 1.55 μm telecommunication windows requires a lower index step and thus a second annealing at 320 °C is applied. After three hours at this temperature the index step has been reduced to a suitable value of 0.0085 with no change in waveguide width. The procedure of using a second annealing enables a standard UV writing process to be applied for a wide variety of structures after which the required index step can be chosen simply by adjusting the annealing time or temperature. An extra benefit of applying a second high temperature annealing is that it removes components of the induced index change that are unstable at normal operating temperatures, thereby yielding devices with a very good degree of long term stability [13].

3. Splitter design

For this work 1×N splitters with N=2,4,8,16,32 have been fabricated, all with the same generic layout. An overview of a 1×16 splitter is shown in Fig. 2(a) while a close-up view of a single Y-branch section is shown in Fig. 2(b). The N-output splitter structure is made by cascading Y-shaped branching sections. The output channel pitch is 127 μm which matches that of commercially available fiber connector arrays. Each branching section is written in three scans, first the access waveguide followed by the two output arms. Each scan starts at the central branching point and moves outwards, as indicated by the arrows in Fig. 2(b).

The use of multiple concatenated scans, as opposed to the dual scanning technique employed in early work [14], enables scalability of a pre-optimized branching section into larger trees. On the other hand it sets stringent requirements on the scanning accuracy, hence the need for interferometric position feedback during the scanning process.

#9482 - $15.00 USD Received 15 November 2005; revised 19 December 2005; accepted 19 December 2005

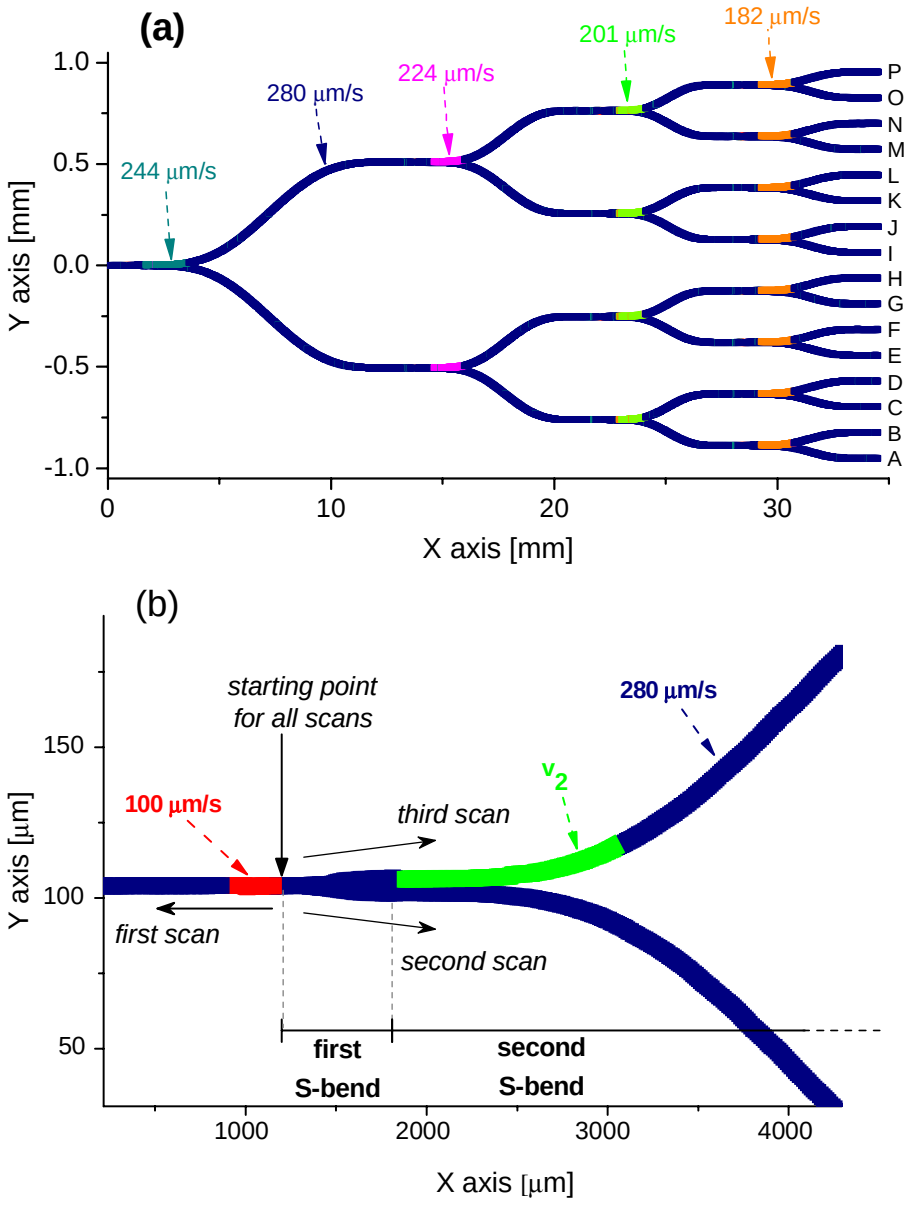

Fig. 2. (a) Overview of a 1×16 splitter layout, with applied scan velocities indicated by arrows. (b) Close-up view of a Y-branch section. On each view the graph colors represent the different scan velocities applied in various sections.

The access waveguide scan begins at 100 μm/s, followed by acceleration to the standard scan velocity of 280 μm/s. A low velocity is used initially to avoid the possibility of irregularities in the waveguide formation process [11]. In order to accurately control the waveguide starting point the delay between the computer command for shutter opening and the actual time of opening (22.9 ms) is taken into account. The combination of high accuracy scanning and shutter delay compensation enables fabrication of junctions with virtually no loss due to misalignment.

#9482 - $15.00 USD Received 15 November 2005; revised 19 December 2005; accepted 19 December 2005

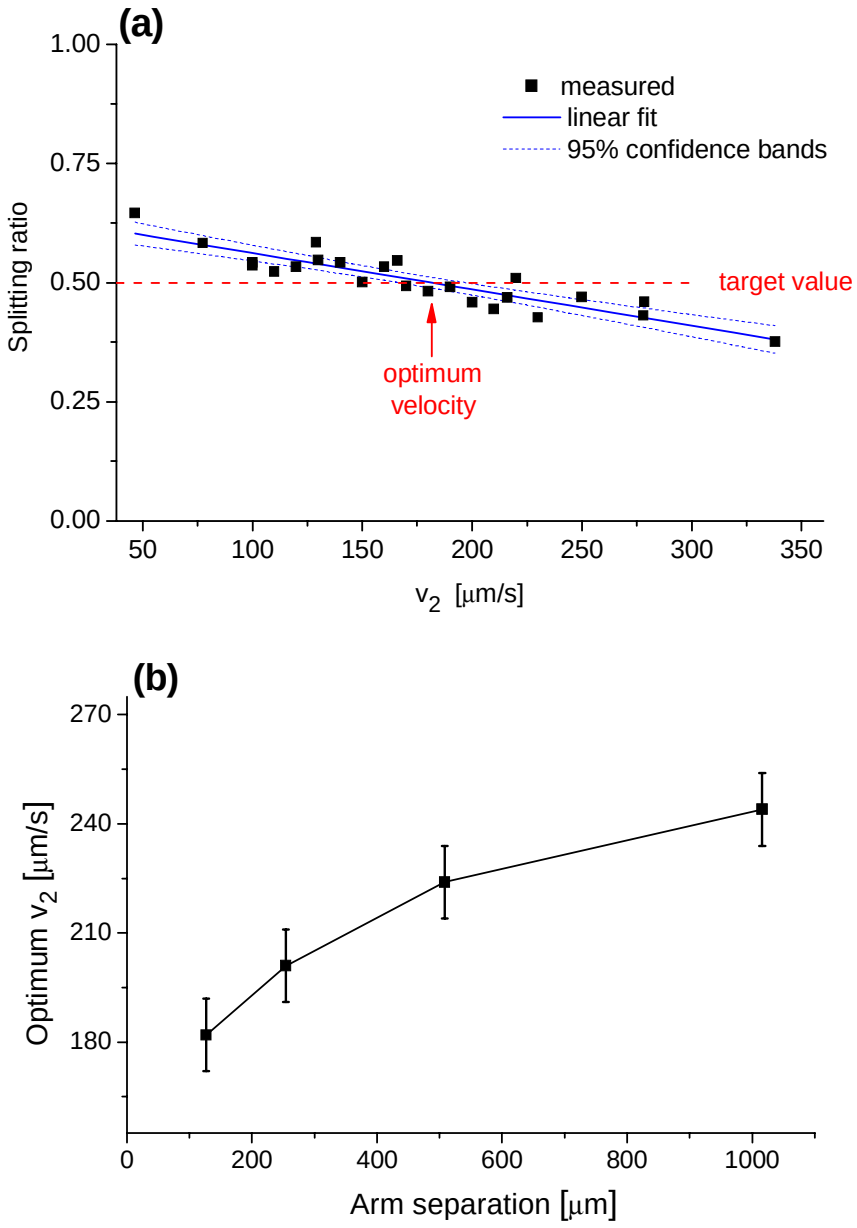

Fig. 3. (a) Measured splitting ratio as a function of the scan velocity v_2 applied on the second arm of a Y branch (see Fig. 2(b)) with an output arm separation 127 μm. A linear fit and confidence bands have been used to determine the optimum v_2 for which a splitting ratio of 50% is achieved. (b) optimum v_2 for different arm separations.

The output arms are shaped as two cascaded polynomial S-bends (Fig. 2(b)). The first S-bend yields a transverse displacement of 6 μm over a length of 700 μm to separate the output arms, so that the combined width at the end of this bend section is twice that of a single waveguide. Hence, an adiabatic taper after the access waveguide is achieved to avoid mode conversion [15]. The second S-bend achieves the required transverse displacement for connecting to the next branching point. Each S-bend is shaped as a 4^{th} order polynomial

#9482 - $15.00 USD Received 15 November 2005; revised 19 December 2005; accepted 19 December 2005

function with null derivatives up to the 3rd order at the boundaries, to reduce mode mismatch with the next access waveguide.

For N=4,8,16 the length of the second bend has been optimized for compactness / low loss and has an equivalent minimum radius of curvature of 20 mm. For N=32 the minimum radius was reduced to 14 mm so that the component could fit our standard chip size. Measurements on (r_{min}=20 mm) concatenated bends with a transverse displacement of 127 μm showed the excess loss to be ~0.05 dB pr. S-bend. The bend loss for the N=32 components is slightly higher, as will be shown later.

If a branching section is written with identical scan velocities in all three scans the resulting splitting ratio will often be asymmetric since the photosensitivity in the vicinity of a UV exposed area [16] can be reduced slightly due to local heating [11]. Symmetrical splitting is achieved by applying slightly different scan velocities in the central part of each branching section [16]. The required scan velocity compensation depends on the length of the section where the two branching waveguides are coupled. For our waveguides this section extends until the center-to-center separation becomes roughly 20 μm. A series of 1×2 splitters were fabricated to determine the velocities required for symmetrical splitting. For an arm separation of 127 μm and a standard scan velocity of 280 μm/s in the first arm, the optimum scan velocity v_2 of the second scan was found to be 180±10 μm/s, as depicted in Fig. 3(a). The datapoint scattering is due to fabrication imperfections and is consistent with a splitting ratio standard deviation of 0.03, which is similar to earlier results [2]. The measured relationship between the optimum scan velocity v_2 and the arm separation is shown in Fig. 3(b). Hence, in order to achieve symmetric splitting throughout a 1×N structure the scan velocity v_2 is chosen according to this relationship, as indicated in Fig. 2(a).

The design outlined above results in total component lengths and fabrication times which are given in Tab. 1. Considering the dimensions of commercial fiber connector arrays, the length of the UV written N=4,8,16 splitters when pigtailed would be reduced by 20–50% in comparison with many commercially available splitters. The production capacity for one scanning station is roughly 40–260 components pr. day depending on the channel count. Since only 45 mW of UV power is required for the writing process one UV laser can power several scanning stations, thereby increasing the production capacity further.

Table 1. Length and UV writing time for the fabricated 1×N splitters

No. of output channels, N	Length [mm]	Fabrication time [s]
4	12.6	314
8	21.5	554
16	34.5	1115
32	(46.0)	(2164)

Note that the N=32 splitter design was forced to fit our standard chip size, hence the associated numbers are placed in parentheses.

4. Performance

To evaluate the component performance and reproducibility several groups of splitters with N=4,8,16,32 were fabricated during a period of ~4 months without any setup maintenance. Each group contained 5–41 individual components, with more components being tested for lower channel counts. In addition to splitters each group contained a few straight reference waveguides.

Device performance was characterized with butt coupled SMF-28 fibers and index-matching oil. A polarized laser source at 1557 nm and a non-polarized supercontinuum

#9482 - $15.00 USD Received 15 November 2005; revised 19 December 2005; accepted 19 December 2005

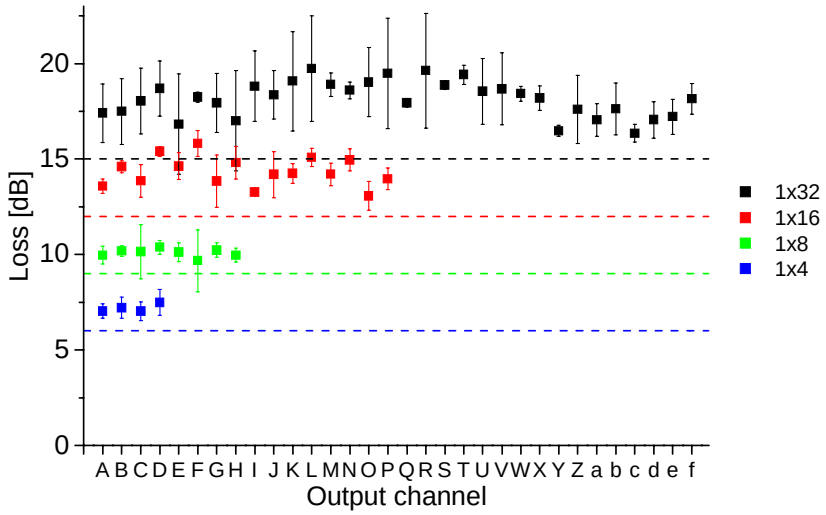

Fig. 4. Insertion loss (symbols) and PDL (bars) measured at 1557 nm for N=4,8,16,32 outputs. The dotted lines indicate the theoretical loss limit corresponding to each type of splitter.

source were used for narrowband and broadband characterization, respectively. The total insertion loss and polarization dependent loss (PDL) at 1557 nm were measured with a dedicated PDL/insertion loss meter, whereas broadband characterization was carried out with an optical spectrum analyzer from 1300–1750 nm. For brevity the following results refer to selected components, although the presented performance is typical for the entire lot.

4.1 Narrowband measurements

On 47 mm long chips the straight reference waveguides exhibited a total insertion loss of 0.4 dB with a PDL at our detection limit of ~0.2 dB. The 1×N splitter performance is summarized in Fig. 4, showing insertion loss and PDL at 1557 nm for each channel. Also shown is the theoretical loss limit of each splitter type, i.e. the loss associated with splitting the input signal into N equal components. The total excess loss for N=4,8,16,32 is 1.2 dB, 1.0 dB, 2.2 dB and 3.0 dB, respectively, which is in agreement with that expected from the initial optimization of bends, branching points, etc. A further improvement can easily be achieved on the 1×32 splitter, which was slightly compressed to fit the chip length used in this work. The splitter uniformity (difference between max. and min. channel loss for a given wavelength) for N=4,8,16,32 is 0.5 dB, 0.7 dB, 2.8 dB and 3.4 dB, respectively. The fact that there is no discernable slope of the channel loss with position shows that there are no significant systematical deviations from symmetrical splitting in the pre-optimized branching points. Since the initial optimization was done several months earlier this shows that the optimum scan velocity, v_2, is quite stable.

The splitter PDL is normally near or just above the detection limit (0.2–0.4 dB), but for some channels it can increase to 1–3 dB. This behavior is seen sporadically in nearly all N=8,16,32 splitters but on different channels each time. Statistics on several hundred IL/PDL measurements show that the occurrence of the problem is correlated with high losses. Hence, for 1×4 splitters the problem is much less severe, to the point of being unnoticeable, and there are in general no PDL problems with 1×2 splitters, bends or long waveguides. This behavior may be caused by interference from vertical modes excited at Y-branch sections and weakly guided in the core layer [17]. Since such modes only contain a small fraction of the total input power the effect only becomes apparent when the light level in the waveguide gets sufficiently low. The use of a core layer with a refractive index before UV exposure which is slightly lower than that of the buffer/cladding will significantly reduce the amplitude of

#9482 - $15.00 USD Received 15 November 2005; revised 19 December 2005; accepted 19 December 2005

weakly guided higher order modes and could thus also reduce the sporadically high PDL. Another cause for the observed behavior may be that the top cladding layer is too thin (small leakage to radiated modes), which would also require an optimization of the sample structure.

4.2 Broadband measurements

The spectral variation of channel loss, uniformity and total excess loss (i.e. overall loss introduced by the device) over a 1300-1750 nm range is depicted in Fig. 5 for the different splitter types. The values at 1557 nm generally agree well with the narrowband measurements presented in Fig. 4. The total excess loss is fairly flat throughout the entire wavelength range, with an average value for N=4,8,16,32 of 1.0 dB, 1.3 dB, 1.6 dB, 3.2 dB, respectively, and a ripple of ~0.5 dB. These losses are comparable to those of currently available commercial components, except for the 1×32 component which has a higher loss due to the previously mentioned deliberate compression of the first bend section.

The channel uniformity for the 1×4 splitters is spectrally flat, with an average value of 1.0 dB and a ripple of 0.2 dB. The 1×8 splitter uniformity is also flat with an average value of 1.0 dB down to 1400 nm, below which it increases to 1.8 dB, most likely due to the approaching multimode behavior. This increase becomes more apparent in the 1×16 and 1×32 splitters. An increase of the post-fabrication annealing temperature will result in a slightly lower waveguide index step and is expected to improve the short wavelength uniformity.

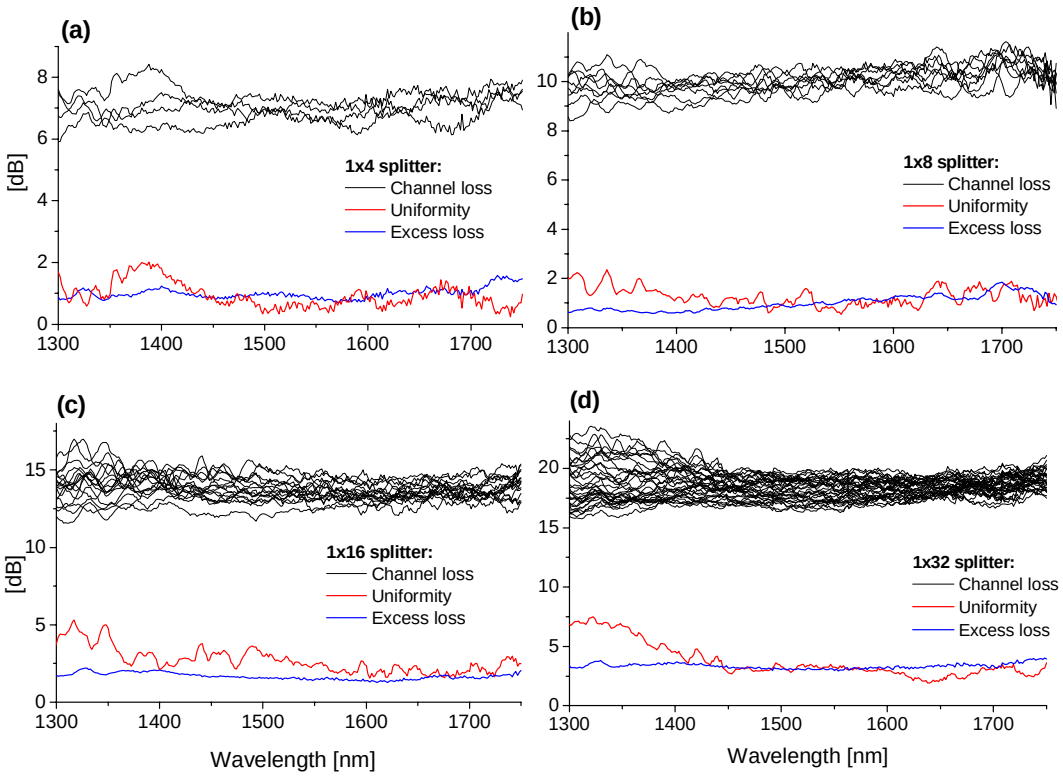

Fig. 5. Spectral variation of insertion loss for each channel, splitter uniformity and total excess loss for: (a) 1×4 splitter, (b) 1×8 splitter, (c) 1×16 splitter, (d) 1×32 splitter.

#9482 - $15.00 USD Received 15 November 2005; revised 19 December 2005; accepted 19 December 2005

5. Conclusion

The first demonstration of 1×N power splitters with N=4,8,16,32 output channels made by direct UV writing has been reported. The components consist of multiple Y-branches, written as concatenated waveguide sections. The demonstrated splitters are compact, and exhibit low excess loss and good uniformity over a wavelength range up to 450 nm. The fabrication process was found to be stable over a period of several months with no setup maintenance. These results indicate that UV writing is a promising technique for fabrication of low-cost splitters for FTTH applications.

#9482 - $15.00 USD Received 15 November 2005; revised 19 December 2005; accepted 19 December 2005